

## **Supporting Information**

of

### **Boric Acid Permeation in Forward Osmosis Membrane Processes: Modeling, Experiments and Implications**

by

Xue Jin<sup>1,2</sup>, Chuyang Y. Tang<sup>1,2,\*</sup>, Yangshuo Gu<sup>1,2</sup>, Qianhong She<sup>1,2</sup>, Saren Qi<sup>1,2</sup>

School of Civil & Environmental Engineering<sup>1</sup> and Singapore Membrane Technology Center<sup>2</sup>

Nanyang Technological University, Singapore, 639798

\* Corresponding author address: Nanyang Technological University; N1-1B-35, 50 Nanyang Avenue; Singapore, 639798; Tel: (65) 67905267; Fax: (65) 67910676; E-mail: [cytang@ntu.edu.sg](mailto:cytang@ntu.edu.sg)

**Number of Pages: 9**

**Number of Figures: 6**

**Number of Tables: 2**

<b>Page 2</b>	<b>S1. Speciation of boric acid;</b>
<b>Page 3</b>	<b>S2. FO membrane structure and surface characteristics;</b>
<b>Page 5</b>	<b>S3. Calculation of experimental Boron Rejection in FO Operation;</b>
<b>Page 7</b>	<b>S4. Experimental results and model predictions for water flux;</b>
<b>Page 8</b>	<b>S5. A comparison between experimental results and model predictions for boron flux;</b>
<b>Page 9</b>	<b>S6. Experimental and predicted boron rejection by CTA-W membrane.</b>

### S1. Speciation of Boric Acid

Boron takes two forms in aqueous solution: non-charged boric acid and negative charged borate ions. The dissociation of boric acid in aqueous solution strongly depends on the water pH (Figure S1). When pH is above 9.25, concentrations of negative charged borate ions become dominant compared to the non-ionic form. At the natural pH level of seawaters (7.9–8.2), boron (95%) is dominantly in the non-ionic boric acid form.

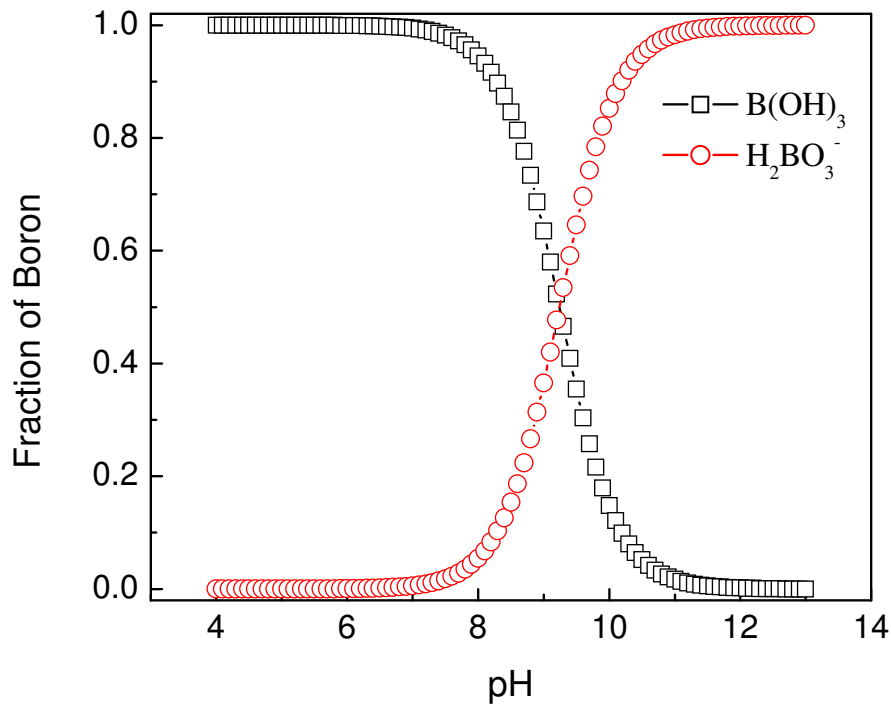


**Figure S1**

Speciation of boric acid in an aqueous solution as a function of the solution pH.

## S2. FO Membrane Structure and Surface Characteristics

SEM micrographs of the CTA-HW and CTA-W membranes are presented in Figure S2. These two images illustrate that both membranes consist of a woven fabric mesh embedded within a continuous polymer layer.

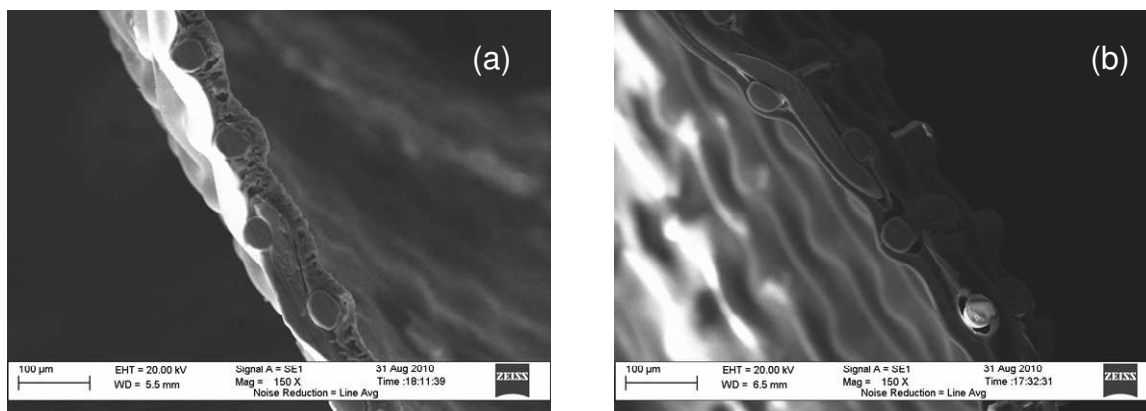


**Figure S2**

SEM micrographs of a cross section of (a) CTA-HW and (b) CTA-W FO membranes

Membrane zeta potentials were determined in a background solution containing 10 mM NaCl using electrokinetic analyzer (SurPASS, Anton Paar, Austria). Membrane hydrophobicity was characterized by sessile drop contact angle measurements with deionized water, using an automated contact angle goniometer (OCA 20, Dataphysics Instruments GmbH, Germany). Membrane samples were dried for 24 h in a dessicator before measuring contact angles.

Zeta potential and contact angel of the FO membranes are reported in Table S1. Based on pure water contact angle data, the active layer of CTA-HW membrane was more hydrophobic while the support layers of both membranes had similar hydrophobicity. At 10 mM NaCl and pH of 6, the active layer and support layer of both membranes exhibited slight negative zeta potentials, but CTA-W was more negatively charged than CTA-HW.

**Table S1**

Membrane surface properties

Membrane	Contact angle (°)		Zeta potential at pH 6 (mV)	
	Active layer	Support layer	Active layer	Support layer
CTA-HW	76.6±0.7	81.8±5.4	-2.1±0.3	-1.5±0.5
CTA-W	69.5±3.9	88.9±3.8	-4.1±0.1	-2.7±0.5

### S3. Calculation of Experimental Boron Rejection in FO Operation

To determine boron rejection, Eq. (14)  $R = 1 - \frac{J_B}{J_w \cdot c_{f,B}}$  require that we know  $J_B$ ,  $J_w$  and  $c_{f,B}$ . These parameters were determined using the following protocol. A new membrane coupon was placed in the cross-flow membrane cell. A 3 L feed solution and a 3 L draw solution were added to the feed and draw solution reservoirs, respectively. Variable speed peristaltic pumps (Cole-Parmer, Vernon Hills, IL) were used to generate cross-flows, forming separate closed loops for the feed and draw solutions. The mass of the feed solution was monitored as a function of time to determine the water flux. It usually took about 30 min for the water flux to stabilize. During FO filtration, the draw solution was continuously diluted by the permeate water. As a result, the apparent driving force decreased at longer filtration time due to the dilution effect, which led to water flux decline. The  $J_w$  used to calculate boron rejection was the average of values from 30 min to 1 hour. Boron concentration in the feed and draw solutions were analyzed by ICP-AES. The  $c_{f,B}$  used to calculate boron rejection was the average of values before and after filtration test. Because the initial boron concentration in the draw solution is zero, a mass balance yields Eq. (18)  $c_{B(t)}(V_{d0} + J_w A_m t) = J_B A_m t$ , where  $c_{B(t)}$  is the experimentally measured boron concentration in draw solution at time  $t$ ,  $V_{d0}$  is the initial volume of draw solution,  $J_w$  is the measured water flux,  $A_m$  is the membrane surface area, and  $t$  is time. The experimental boron flux,  $J_B$ , was obtained from the slope of plotted  $\frac{c_{B(t)}(V_{d0} + J_w A_m t)}{A_m}$  versus  $t$  (Figure S3). In all cases investigated in this study, boron permeation flux was not affected by the concentration changes in feed and draw solutions during filtration.

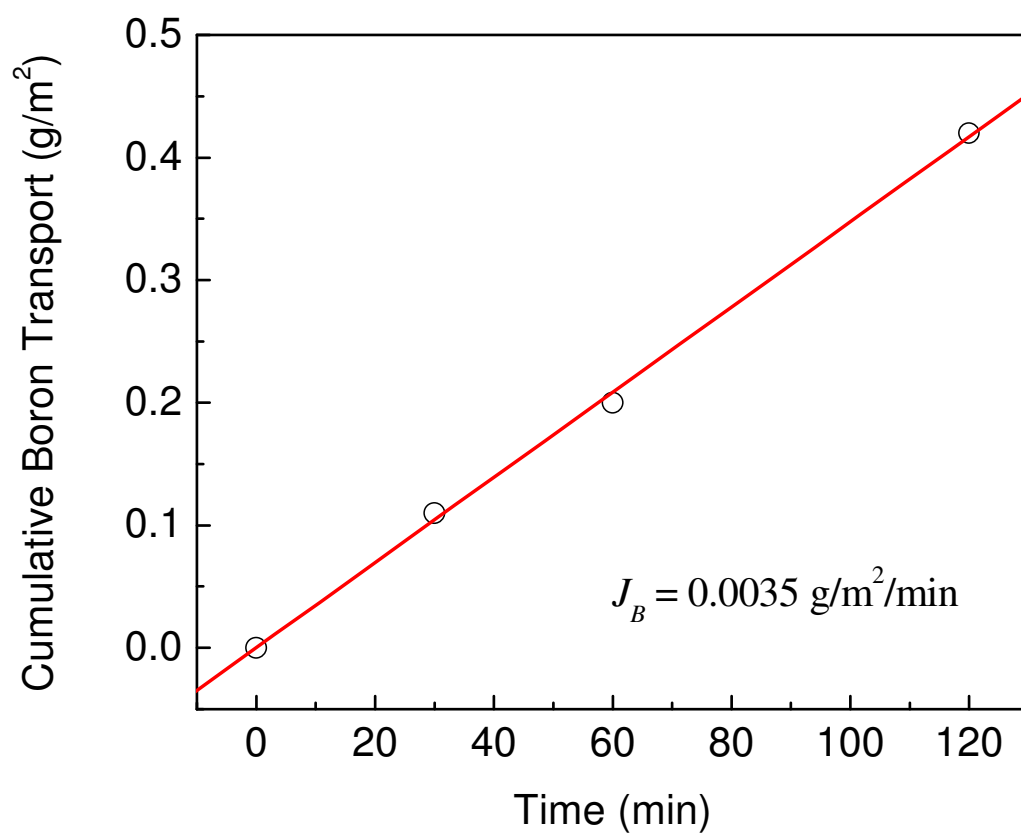


**Figure S3**

Cumulative boron transport in the draw solution versus time

#### S4. Experimental Results and Model Predictions for Water Flux

Figure S4 presents the experimental determined and model predicted water fluxes. The predicted values were calculated using Eqs. (3) and (4) for the AL-FW and AL-DS orientations, respectively. Values for the transport parameters in the two equations were showed in Table S2.

The predicted water flux did not perfectly match with experimental water flux when feed water was composed of 0.5 M NaCl and active layer was facing draw solution (AL-DS). Therefore, the experimental water flux was used instead of model predicted value to predict boron flux in this study because of the physical insights our model can provide. In our future study, more complex models including predicted water flux will be developed.

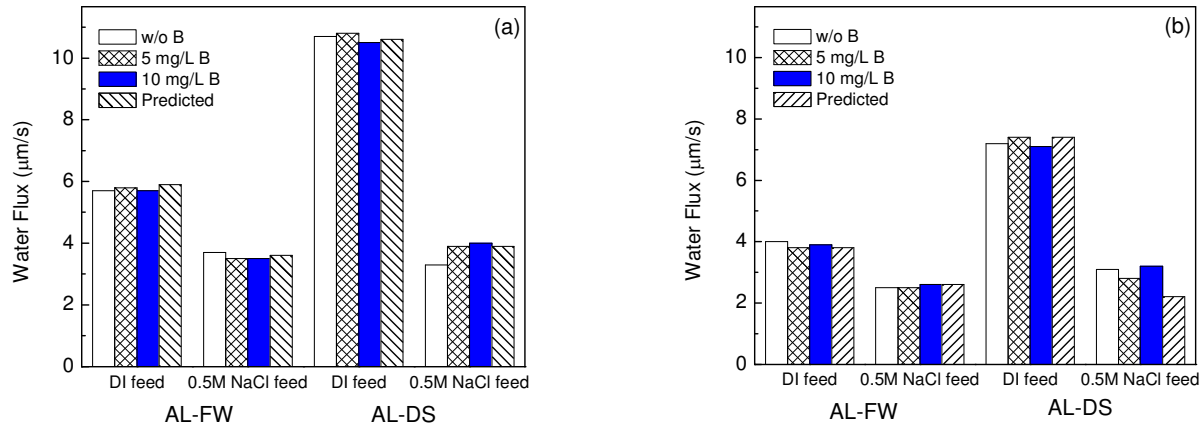


**Figure S4**  
Experimental and predicted water fluxes.

**Table S2**  
Membrane transport parameters

Membrane	Water permeability	NaCl permeability	NaCl Mass Transfer Coefficient, $K_{m,s}$ (m/s)	
	$A$ , (m/s·Pa)	$B_s$ , (m/s)	AL-FW	AL-DS
CTA-HW	$2.55 \times 10^{-12}$	$2.72 \times 10^{-7}$	$4.05 \times 10^{-6}$	$2.73 \times 10^{-6}$
CTA-W	$1.07 \times 10^{-12}$	$6.45 \times 10^{-8}$	$3.85 \times 10^{-6}$	$1.94 \times 10^{-6}$

### S5. A Comparison between Experimental Results and Model Predictions for Boron Flux

Figure S5 compares the boron fluxes produced by model predictions and experimental measurements. The predicted values were calculated using the  $B_B$  and  $K_{m,B}$  values determined in Sections 4.1-4.2 and the experimentally measured water fluxes given in Figures 3a and 3b. In general, there is a strong agreement between modeling results and experimental data. This indicates that the models developed in this study, which incorporates both operating parameters (orientation and water flux) and membrane characteristics, can be use as a reliable predictor for boron transport during FO processes.

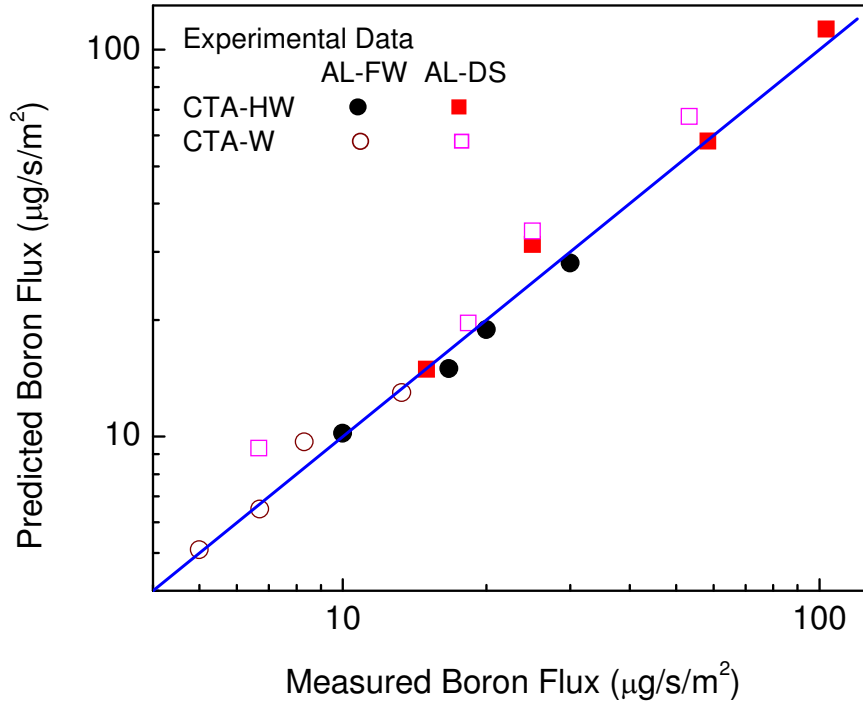


**Figure S5**

A comparison of experimental results and model predictions for boron flux. The solid line (slope = 1) represents perfect agreement between experimental data and model predictions.



### S6. Experimental and Predicted Boron Rejection by CTA-W Membrane

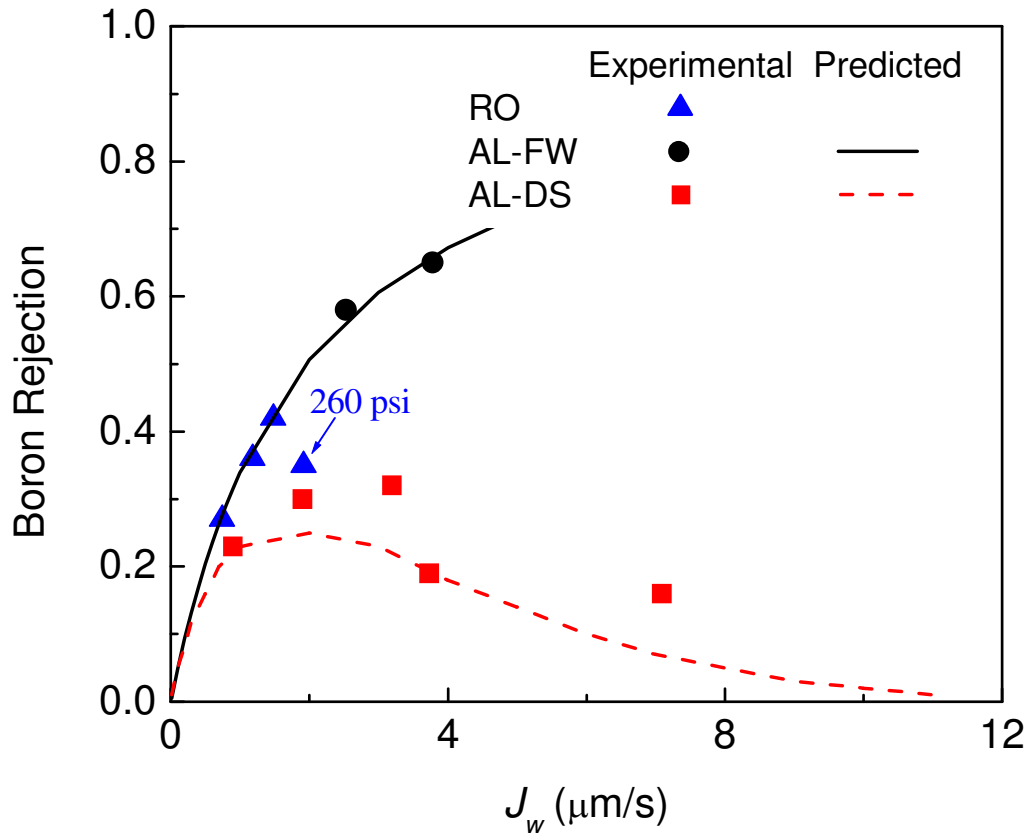


**Figure S6**

Observed and predicted boron rejection by CTA-W membrane as a function of water flux with various operation modes. The feed solution contained 5 mg B/L in DI water. Other experimental conditions were as follows: cross-flow velocity = 23.2 cm/s, pH  $\approx$  6, and temperature = 24 °C. The permeate flux was varied by changing the applied pressure (60-260 psi) for RO operation and by changing NaCl concentration (0.2-2 M) in draw solution.